Available online at www.sciencedirect.com
ScienceDirect
Journal of Power Sources 164 (2007) 472–480
JOURNAL OF POWER SOURCES
www.elsevier.com/locate/jpowsour

Synthesis and activation of Pt nanoparticles with controlled size for fuel cell electrocatalysts

Zhufang Liu [a], Mohammad Shamsuzzoha [b], Earl T. Ada [b], W. Matthew Reichert [a], David E. Nikles [a,*]

[a] *Department of Chemistry, The University of Alabama, Tuscaloosa, AL 35487-0336, USA*
[b] *Central Analytical Facility, The University of Alabama, Tuscaloosa, AL 35487-0336, USA*

Received 13 September 2006; received in revised form 19 October 2006; accepted 23 October 2006
Available online 27 December 2006

Abstract

Well-dispersed Pt nanoparticles with controlled size and narrow size distribution were prepared by polyalcohol reduction of platinum acetylacetonate, using oleylamine as a capping agent. The particle size was varied from 3.5 nm to 11.5 nm by decreasing the amount of oleylamine added in the synthesis. Size selection of the as-prepared particles by solvent fractionation yielded nearly monodispersed Pt particles. The as-prepared particles were loaded on a carbon support by physical deposition, but showed no electrocatalytic activity due to the oleylamine bound to the particle surface. The particles were activated for electrocatalysis after heating the particles in air at 185 °C for 5 h, conditions that gave no particle-sintering and no oxidation. Cyclic voltammetry showed that the particles after the heat treatment in air were electrocatalytically active for methanol oxidation. The smaller 3.5 nm and 4.0 nm Pt particles had a higher intrinsic activity for methanol oxidation, but a lower tolerance to CO poisoning, compared with 6.0 nm, 9.5 nm and 11.5 nm particles. CO-stripping results suggest that CO is more easily oxidized on larger Pt particles.

Keywords: Platinum nanoparticles; Oleylamine; Controlled size; Heat treatment; Catalytic activity; Methanol oxidation

1. Introduction

Fuel cell technology is a very promising energy source due to its low pollutant-emission and high energy-conversion efficiency. Carbon-supported Pt nanoparticles remain the choice for electrocatalysts of fuel cells, because of their electrocatalytic activities for both the oxidation of hydrogen and methanol on the anode and the reduction of oxygen on the cathode. It is known that the catalytic activity of particles is dependent on the particle size, shape, size distribution and dispersion [1–5]. Therefore, it is of great significance to develop a synthetic method through which well-dispersed Pt nanoparticles with tunable size and narrow size distribution can be made. Many methods have been employed to prepare carbon-supported Pt nanoparticles, including wet impregnation [6–9], electrochemical deposition [10–12] and surfactant or ligand-based colloidal methods [13,14]. In the conventional impregnation approaches, Pt particles are directly deposited on carbon supports during the chemical reduction of Pt precursors by reducing agents, such as H_2 or $NaBH_4$. This is a simple and one-step preparation method, but it provides a poor control over the particle size and size distribution, especially for the preparation of high-loading (higher than 30%) Pt catalysts. Electrochemical deposition offers another simple routine to directly prepare Pt particles on carbon substrates, but reducing the particle size down to 5 nm is still a big challenge for this method. Recently, surfactant or ligand-based colloidal methods for Pt particle preparation have attracted more and more attention. One of the desirable features associated with this approach is that the particle size, size distribution and even the dispersion can be simply controlled by the capping agent used in synthesis. For catalysis application, the as-prepared particles then can be deposited on various carbon supports, such as carbon powder or carbon nanotube. However, the carbon-supported as-prepared particles are catalytically inactive owing to the capping agents bound to the particle surface and treatments are always required to remove the capping agent attaching the particle surface, activating the catalytic activity of Pt particles. Conventional methods used for removing capping agents

* Corresponding author. Tel.: +1 205 348 8445; fax: +1 205 348 9104.
E-mail address: dnikles@mint.ua.edu (D.E. Nikles).

0378-7753/$ – see front matter © 2006 Elsevier B.V. All rights reserved.
doi:10.1016/j.jpowsour.2006.10.104

are high-temperature calcinations in inert atmosphere, but these high-temperature treatments may induce the sintering of particles [14], causing the loss of surface area and consequently the degradation of catalytic activity. Thus, to obtain Pt catalysts with maximized catalytic activity, non-thermal or low-temperature heat treatments need to be developed, provided appropriate capping agents are selected.

In this study, we reported a novel method for Pt nanoparticle synthesis and activation. Pt nanoparticles with controlled size and narrow size distribution were prepared by polyalcohol reduction of platinum acetylacetonate with the presence of oleylamine and a simple size selection method was developed to further narrow the size distribution of particles. Physical deposition was employed to deposit as-prepared particles on XC-72 carbon support. For particle activation, three different approaches were tried to remove the oleylamine bound to particle surface. The size-dependent electrocatalytic activity for methanol and CO oxidation of activated Pt catalysts was investigated using cyclic voltammetry (CV) and CO-stripping voltammetry.

2. Experimental

2.1. Materials

Platinum acetylacetonate ($C_{10}H_{14}O_4Pt$, 97%), 1,2-hexadecanediol ($C_{16}H_{34}O_2$, 90%), oleylamine ($C_{18}H_{37}N$, 70%), diisopentyl ether ($C_{10}H_{22}O$, 99%) and Nafion® (5 wt.%) were purchased from Aldrich. Diphenyl ether ($C_{12}H_{10}O$, 70%) was from Acros Organic. Other chemicals, including ethanol, methanol (HPLC grade), acetone, hexane and sulfuric acid were purchased from Fisher Scientific. Vulcan XC-72 carbon powder was a gift from Cabot Inc. All the chemicals were used as received. Millipore water was used to prepare aqueous solutions.

2.2. Synthesis of Pt nanoparticles

Taking the preparation of 3.5 nm Pt nanoparticles as an example, 95.0 mg platinum acetylacetonate, 390.0 mg 1,2-hexadecanediol and 20 ml diphenylether were added into a 50-ml round flask equipped with magnetic stir and a reflux condenser. The mixture then was heated from room temperature to 110 °C at a rate of 5 °C min^{-1} under N_2 atmosphere. The resulting brown solution was held at 110 °C for 2 min, during which 1.36 ml of oleylamine was injected drop wise by syringe. The mixture was then heated to 175 °C with the same heating rate and was kept at this temperature for 1 h. Afterwards, the obtained black particle dispersion was allowed to cool down to 50 °C and then transferred to a glass tube containing 20.0 ml ethanol, followed by 5 min sonication. Then, the yellow-brown supernatant was discarded and the remaining particle dispersion was transferred to a centrifugation tube containing 5.0 ml ethanol. Particles were isolated by centrifugation and finally dispersed in hexane, making an as-prepared Pt particle dispersion (~3.8 mg ml^{-1}). 4.0 nm, 6.0 nm, 9.5 nm and 11.5 nm particles were prepared by the same procedure, except that 0.68 ml, 0.34 ml, 0.17 ml and 0.08 ml of oleylamine were added, respectively, during the synthesis.

2.3. Narrowing the size distribution of as-prepared Pt particles

The size distribution of as-prepared particles was further narrowed by a simple size selection method. The detailed procedures for this method can be described as follows. Briefly, 5.0 ml ethanol was added into 3.0 ml as-prepared Pt particle dispersion mentioned above and the resulting mixture was sonicated for 10 min. Due to the hydrophobic nature of particle surface and the mass difference, the larger particles were easier to precipitate than the smaller particles and finally were isolated at the bottom of centrifuge tube after 5 min centrifugation (2000 rpm). The remaining yellow dispersion of smaller particles was collected. By this way, the size distribution of particles can be narrowed and nearly monodispersed Pt particles with different size can be gradually separated with the repetition of this procedure.

2.4. Loading Pt nanoparticles on Vulcan XC-72 carbon support and removing the capping agent

To make carbon-supported 3.5 nm, 4.0 nm, 6.0 nm, 9.5 nm and 11.5 nm Pt catalysts with 40% loading, 15.6 mg as-prepared Pt particles dispersed in hexane were first mixed with 23.4 mg XC-72 carbon powder. Particles were deposited on carbon support by sonicating the resulting mixture for 2 h. The carbon-supported particle dispersion then was dried at 60 °C under air atmosphere with the evaporation of hexane. To activate the catalytic activity of as-prepared particles supported on carbon, three different treatments were employed: (1) heat treating the particles in a tube furnace at 185 °C for 5 h under air atmosphere, (2) heat treating the particles in a tube furnace at 400 °C for 5 h under the Ar/H_2 atmosphere (5% of H_2) and (3) exposing the particles to UV/ozone in a UVO-CLEANER for 1 h.

2.5. Characterization

The X-ray diffraction patterns (θ–2θ scan) of particles were obtained on a Rigaku model D/MAX-2BX thin film diffractometer with a Cu Kα X-ray source (1.5406 Å). The samples were prepared by dropping 0.2 ml particle dispersion on p-type silicon substrates (1 cm × 2 cm) followed by the evaporation of solvents at room temperature. TEM images of samples were obtained on a Hitachi 8000-200 kV transmission electron microscope. The TEM samples were made by placing several drops of dilute particle dispersion on carbon-coated copper TEM grids (400-mesh from SPI). Thermal gravimetric analysis (TGA) was performed on a TA Instruments (Model 2950, New Castle, DE) and 7.4 mg oleylamine in Pt pan was heated from room temperature to 250 °C under air atmosphere with a heating rate of 5 °C min^{-1}. X-ray photoelectron spectroscopy (XPS) was used to determine the oxidation states of Pt particles and check whether oleylamine has been removed from particle surface after different treatments. The spectra were collected on a Kratos AXIS 165 multi-technique electron spectometer, using Mg Kα (1486.6 eV)

as X-ray source. The binding energy of samples was referenced to the C 1s peak (285.0 eV). The samples for XPS characterization were prepared by depositing several drops Pt particle dispersion on silicon substrates followed by the evaporation of solvents. Fourier transform infrared (FT-IR) measurements, complementing to the XPS data, were carried out on a FT-IR spectrometer (Bio-Rad, FTS-40), which was used to determine if the oleylamine has been removed from the Pt particle surface after the heat treatment in air. The particle dispersion was cast on ZnSe lens (25 mm diameter, 2 mm thick) and then were directly used for analysis after the evaporation of hexane.

To investigate the catalytic activity of particles, electrochemical characterization (CV) was performed on a bipotentiostat (AFCBP1, Pine Instrument) with a three-electrode electrochemical cell. The working electrode was prepared in following procedures according to the literature reports [14–16] with minor changes: a glassy carbon (GC) electrode (BAS, 3 mm diameter) was first polished using alumina powder with sizes of 5 μm, 1 μm and 0.05 μm, followed by 2-min sonication in water and acetone. 15.6 mg carbon-supported Pt particles were mixed with 400 μl Nafion® (5 wt.%) and 4.0 ml millipore water to make Pt catalyst ink (~3.5 mg Pt ml^{-1}) and 2 μl catalyst slurry was cast on the polished GC electrode by a micro-pipette. The catalyst ink then was dried at 60 °C in a vacuum furnace. Pt wire and saturated calomel electrode (SCE) were used as a counter and reference electrode, respectively. The electrolytes were bubbled with N_2 gas for 30 min before analysis. In CO-stripping voltammetry, CO was adsorbed on particles by dosing CO gas at the potential of 60 mV (versus SCE) for 5 min. The CO dissolved in electrolytes was displaced by continuously bubbling the solution with N_2 for 30 min.

3. Results and discussion

3.1. Synthesis of Pt nanoparticles with controlled size.

Representative TEM images of as-prepared Pt particles with the size of 3.5 nm, 4.0 nm, 6.0 nm, 9.5 nm and 11.5 nm are shown in Fig. 1(a–e). As shown in Fig. 2, all the particles display a narrow size distribution and a good dispersibility in hexane. Fig. 3 shows the XRD patterns of as-prepared Pt particles synthesized by using different amounts of oleylamine. It can be seen that all the particles have a face-centered cubic (fcc) phase and both the (1 1 1) and (2 0 0) peak becomes broader with the increasing amount of oleylamine. Therefore, varying the amount of oleylamine provides a simple way to tune the particle size, utilizing its covalent bonding with Pt surface. The particle size was tuned to 3.5 nm, 4.0 nm, 6.0 nm, 9.5 nm and 11.5 nm, respectively, when 1.36 ml, 0.68 ml, 0.34 ml, 0.17 ml and 0.08 ml oleylamine were added in 20.0 ml diphenyl ether during the synthesis. The particle sizes were estimated based on both Scherrer's equation and TEM analysis. Table 1 summarizes the TEM-based average particle size and standard deviation of as-prepared particles shown in Fig. 1(a–e), compared with average particle size estimated from XRD Scherrer analysis. It is evident that the average particle sizes from these two approaches are in good agreement.

Table 1
Average particle size and standard deviation of as-prepared Pt particles shown in Fig. 1(a–e), with a comparison with average particle size obtained from XRD Scherrer analysis

As-prepared Pt particles	TEM		XRD
	Average particle size (nm)	Standard deviation (nm)	Average particle size (nm)
(a)	3.5	0.58	3.5
(b)	4.0	0.85	3.9
(c)	6.0	0.73	5.9
(d)	9.5	0.67	9.4
(e)	11.5	0.73	11.4

3.2. Narrowing the size distribution of as-prepared Pt particles

It was interesting to find the size distribution of as-prepared particles could be narrowed by the simple size selection method described in the experimental section. Fig. 4(a) is the TEM image of Pt particles obtained after one size selection procedure, using the particles shown in Fig. 1(b) as original particles. Comparing the size distribution curves of particles after size selection (Fig. 4(b)) and that of original particles (Fig. 2(b)) indicates the size distribution of particles was apparently narrowed after size selection. The average particle size decreased from 4.0 nm to 3.5 nm and particle size standard deviation was reduced from 0.85 nm to 0.50 nm. In fact, the size distribution can be further narrowed if more size selections are performed. These nearly monodispersed Pt particles are desirable materials for studying the size-dependent behaviors of Pt nanoparticles.

3.3. Removing the capping agent bound to particle surface

In the synthetic procedure described above, oleylamine plays a crucial role in controlling the particle size and stabilizing the particles. However, it should be noted that it also blocks the active surface sites of Pt particles. Based on the thermal properties of oleylamine, three different approaches were tried to remove the oleylamine off the particle surface. Fig. 5 shows the high-resolution XPS spectra (N 1s) of 4.0 nm Pt particles after three different treatments in a comparison with as-prepared particles. It was found that oleylamine could be removed from particle surface by both of the two thermal treatments (in air at 185 °C and in Ar/H_2 at 400 °C). While, unfortunately the UV/ozone treatment does not work. Fig. 6 contains the TEM images and size distributions of carbon-supported 4.0 nm Pt particles (40% loading) after the two heat treatments mentioned above. It is clear that the particles still retained their initial size and exhibited a narrow size distribution (Fig. 6(a and c)) after the heat treatment in air at 185 °C. However, there was considerable particle sintering and size-distribution broadening after the heat treatment in Ar/H_2 at 400 °C (Fig. 6(b and d)). Thus, the low-temperature treatment is a more favorable particle activation approach compared with the high-temperature treatment, because high-temperature treatment causes particle sintering and consequently degrades the catalytic activity of particles. In

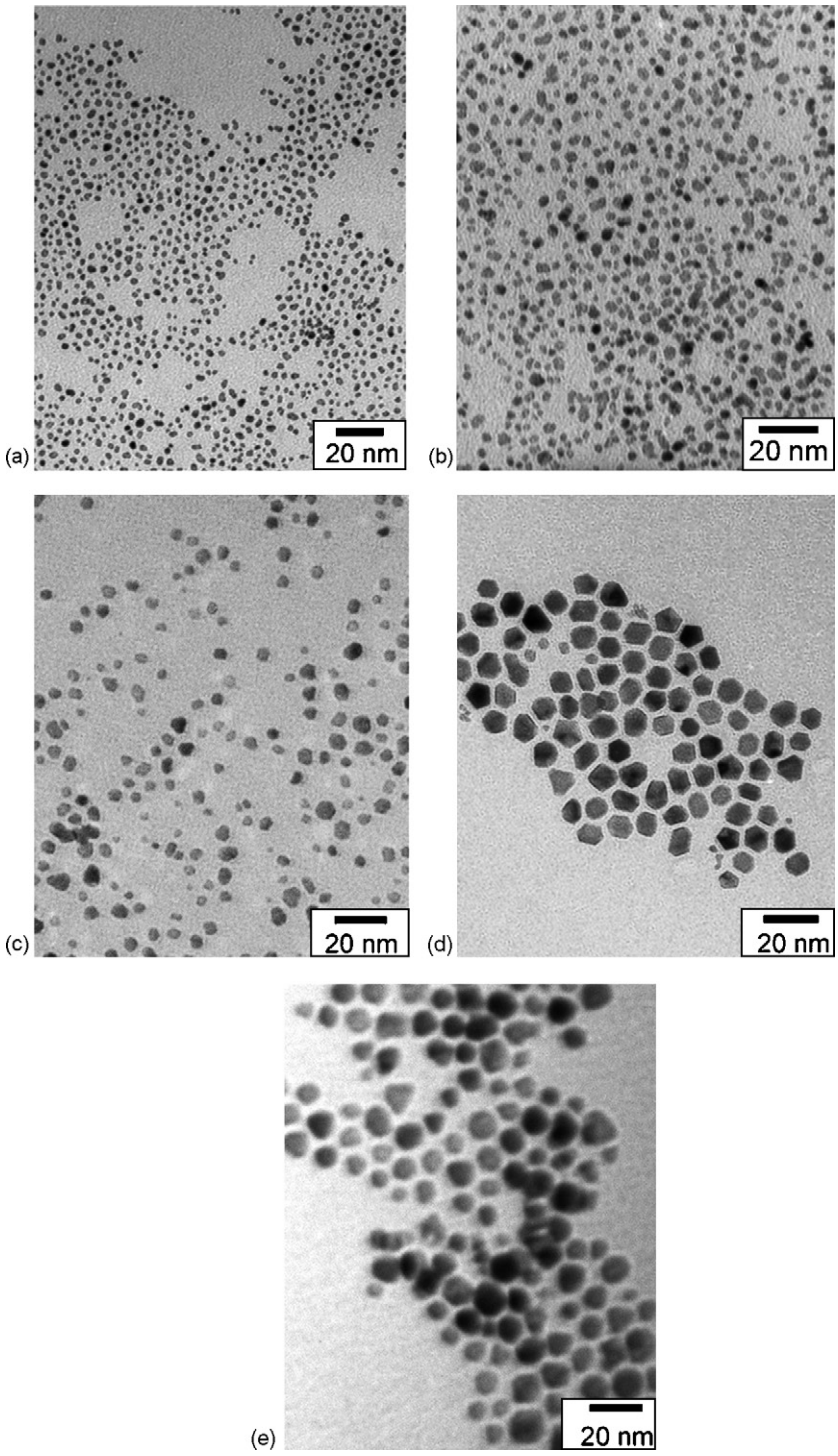

Fig. 1. TEM images of as-prepared Pt nanoparticles with different size: (a) 3.5 nm, (b) 4.0 nm, (c) 6.0 nm, (d) 9.5 nm and (e) 11.5 nm.

this report, to obtain Pt catalysts with maximized catalytic activity, the low-temperature treatment (185 °C in air) was finally selected as the activation approach for oleylamine-capped Pt particles.

Fig. 7 contains the XRD patterns of carbon-supported Pt particles (3.5 nm, 4.0 nm, 6.0 nm, 9.5 nm, 11.5 nm) after the heat treatment in air at 185 °C for 5 h. It was found that there is no significant grain growth of particles after this heat treatment, which demonstrates one of the most appealing features associated with this low-temperature activation approach. The TGA curve of liquid oleylamine shown in Fig. 8 suggests the oleylamine can be burned off particle surface at 185 °C in air atmosphere. This was expected since the flashing point of oleylamine in air is around 160 °C. The FT-IR spectra of particle dispersion (Fig. 9) further confirmed that most of oleylamine was removed after the heat treatment in air. The peaks associated

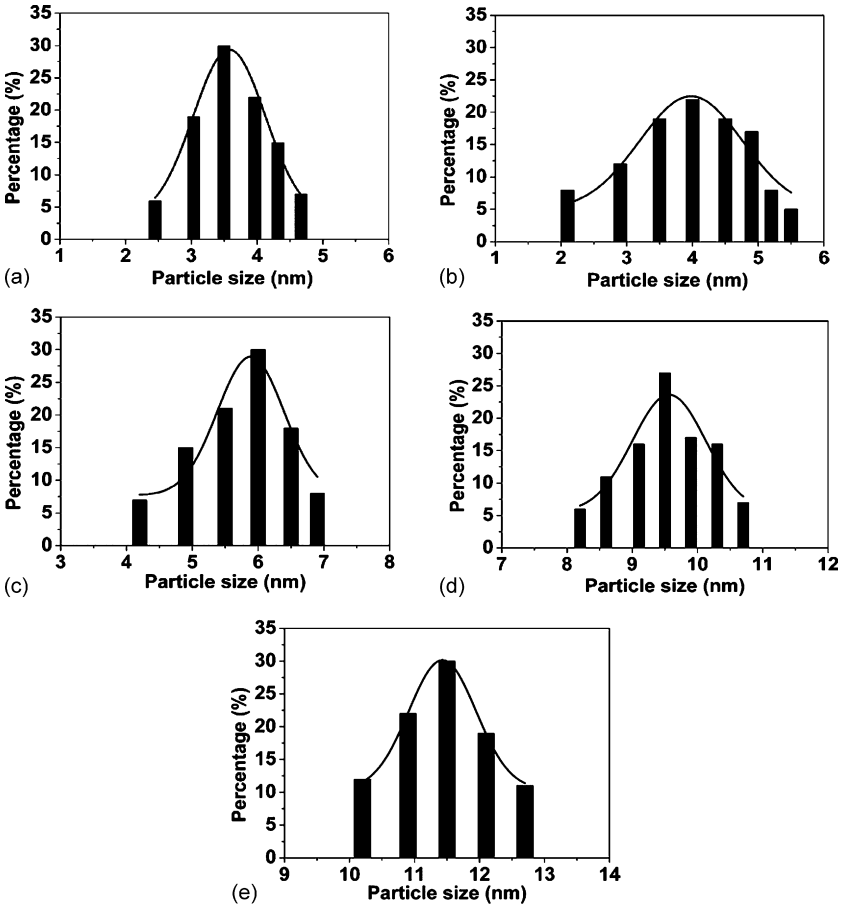

Fig. 2. Size distributions of as-prepared Pt nanoparticles shown in Fig. 1: (a) 3.5 nm, (b) 4.0 nm, (c) 6.0 nm, (d) 9.5 nm and (e) 11.5 nm. The histograms were obtained by measuring 300 randomly selected particles.

with NH (~3300 cm^{-1}) and –HC = (~3006 cm^{-1}) disappeared in the sample after the heat treatment in air at 185 °C for 5 h and the absorbance associated with C–H stretch of alkyl group also dramatically decreased. The low absorbance of alkyl group was likely attributed to the residues yielded during the heat treatment.

XPS was employed to determine the surface oxidation states of Pt particles after the heat treatment in air. Fig. 10 shows the high-resolution scan of Pt 4f for 4.0 nm Pt particles after the heat treatment in air at 185 °C. The peak positions for Pt $4f_{7/2}$ and Pt $4f_{5/2}$ were approximately at 71.7 eV and 75.2 eV, which are slightly higher than that of bulk Pt. This positive shift of binding energy may be resulted from the small size of particles [17], so there is no apparent oxidation for the particles after the treatment in air.

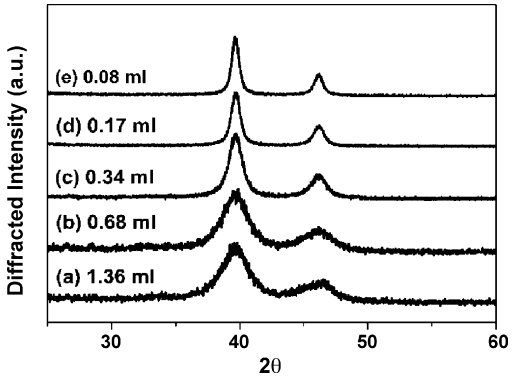

Fig. 3. XRD patterns of as-prepared Pt nanoparticles made by using different amounts of oleylamine: (a) 1.36 ml, (b) 0.68 ml, (c) 0.34 ml, (d) 0.17 ml and (e) 0.08 ml.

3.4. Electrocatalytic activity of Pt particles with different size

The electrocatalytic activity of the carbon-supported particles was characterized by CV, which is a convenient tool in electrochemistry. As we expected, the as-prepared 4.0 nm Pt particles exhibits no electrocatalytic activity in H_2SO_4 (Fig. 11(a)) and no hydrogen adsorption/desorption was shown. This was mainly attributed to the oleylamine bound to the Pt particle surface, which blocked the active sites of particles. However, for the 4.0 nm particles after the heat treatment in air at 185 °C for 5 h, a cyclic voltammogram (Fig. 11(b)) which is similar to that of polycrystalline Pt electrodes was obtained and the adsorption/desorption of weakly and strongly bound hydrogen was clearly observed, implying that the particles have been catalytically activated after the heat treatment in air.

The surface area of Pt catalysts was estimated by integrating the charge under hydrogen underpotential deposition (UPD) region in cyclic voltammograms of Pt particles in H_2SO_4 solu-

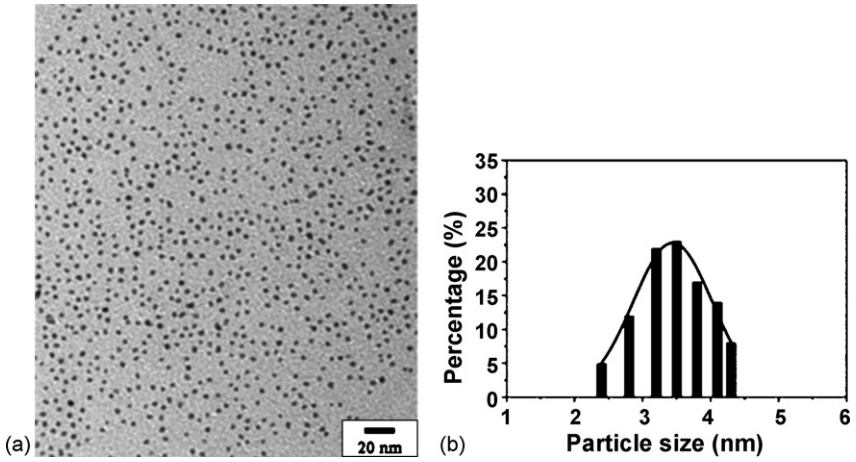

Fig. 4. (a) TEM image and (b) size distribution of Pt nanoparticles obtained after one size selection procedure, using the particles shown in Fig. 1(b) as the original particles.

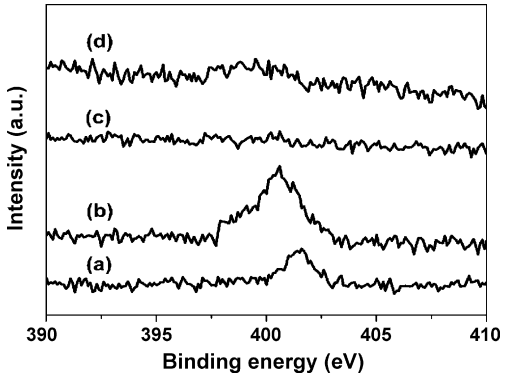

Fig. 5. X-ray photoelectron spectra (N 1s) of 4.0 nm Pt particles: (a) as-prepared, (b) after exposure to UV/ozone for 1 h, (c) after heat treatment in Ar/H_2 at 400 °C for 5 h and (d) after heat treatment in air at 185 °C for 5 h.

tion, presuming that the charge of 0.21 mC is approximately corresponding to the surface area of 1 cm^2 [18]. Table 2 contains the particle sizes and standard deviation of activated Pt/C particles from TEM and XRD analysis and also the surface area estimated from CV experiments. It can be seen that the activated Pt/C catalysts with 40% loading display a narrow particle size distribution and the average particle size from TEM is in good agreement with that from Scherrer analysis. The size distribution of the particles is slightly broader than that of the state-of-art of Pt/C catalysts [19], however, it should be pointed out that these activated Pt/C catalysts are prepared from as-prepared Pt particles without any size selection. If the as-prepared particles after one size selection, such as particles shown in Fig. 4(b), are used as original materials, nearly monodispersed activated Pt/C catalysts could be obtained. Furthermore, this simple size selection process could be repeatedly performed to prepare monodispersed Pt/C catalysts after thermal treatment. In addition, the surface area of activated Pt/C, which decreases with the increasing of particle size, is comparable with that of the state-of-art catalysts.

Fig. 12 shows the cyclic voltammograms of activated carbon-supported Pt particles with different size in 1.0 M H_2SO_4 solution containing 2.0 M CH_3OH. The current density was normalized to mA cm^{-2}. We can find all the particles exhibit certain magnitude of catalytic activity for methanol oxidation. However, the normalized current density of smaller particles (3.5 nm and 4.0 nm particles) is much higher than that of larger particles (6.0 nm, 9.5 nm and 11.5 nm particles), suggesting small-size Pt particles have higher intrinsic catalytic activity for methanol oxidation. In the cyclic voltammograms of methanol oxidation, the forward anodic peak and reverse anodic peak are associated with the oxidation of methanol and carbonaceous species, respectively, and the ratio of forward anodic peak current (I_f) to the reverse anodic peak current (I_b) can be employed to evaluate particles' tolerance of carbonaceous species. A high I_f/I_b value suggests a high tolerance to carbonaceous species, especially for CO [16]. In Fig. 12, it is discernible that the value of I_f/I_b increases with the increasing of particle size, implying big-size

Table 2
Average particle size and standard deviation of activated Pt/C particles with a comparison with average particle size estimated from XRD Scherrer analysis, and the surface area derived from cyclic voltammetry experiments

Activated Pt/C particles	TEM		Average particle size from Scherrer analysis (nm)	Surface area estimated from CV experiments ($m^2\,g\,Pt^{-1}$)
	Average particle size (nm)	Standard deviation (nm)		
(a)	3.6	0.59	3.7	72
(b)	4.1	0.81	3.9	65
(c)	6.0	0.75	5.9	40
(d)	9.5	0.68	9.8	30
(e)	11.5	0.72	12.0	23

(a–e) are corresponding to the activated Pt/C particles prepared from as-prepared Pt particles shown in Fig. 1(a–e), respectively.

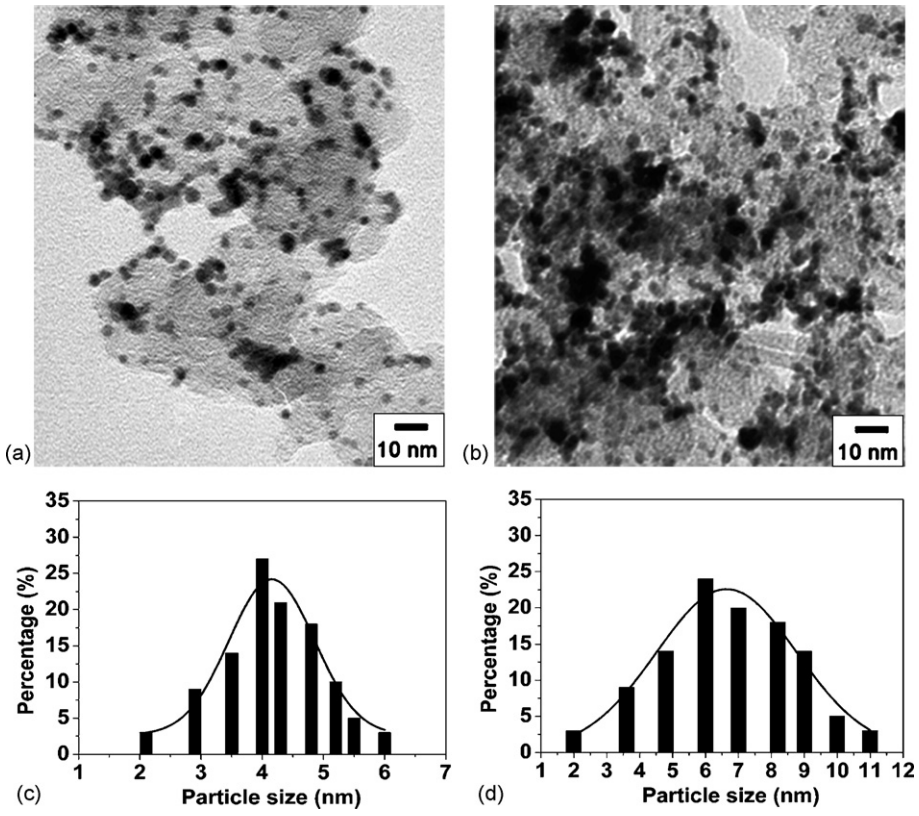

Fig. 6. TEM images and size distributions of carbon-supported 4.0 nm Pt particles (40% loading) after heat treatments: (a and c) in air at 185 °C for 5 h and (b and d) in Ar/H_2 at 400 °C for 5 h.

particles exhibit higher tolerance to the poisoning of CO than the small-size particles. It is possible that the high intrinsic activity of small-size particles for methanol oxidation comes from their high activity for methanol dehydrogenation step.

Fig. 13 shows the anodic CO-stripping curves of particles with different size. Prior to the oxidation of adsorbed CO, the hydrogen adsorption/desorption is completely suppressed; but after the removal of adsorbed CO, the peak associated with hydrogen adsorption appears. More interestingly, the peak for adlayer CO oxidation was found to negatively shift with the increasing of particle size, that is, preadsorbed CO is easier to be oxidized on larger particles than on smaller particles. This

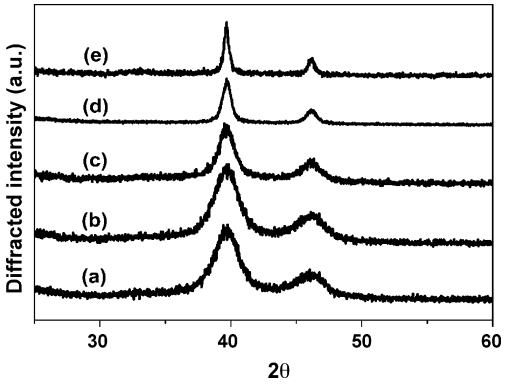

Fig. 7. XRD patterns of Pt particles after heat treatment in air at 185 °C for 5 h: (a) 3.5 nm particles, (b) 4.0 nm particles, (c) 6.0 nm particles, (d) 9.5 nm particles and (e) 11.5 nm particles.

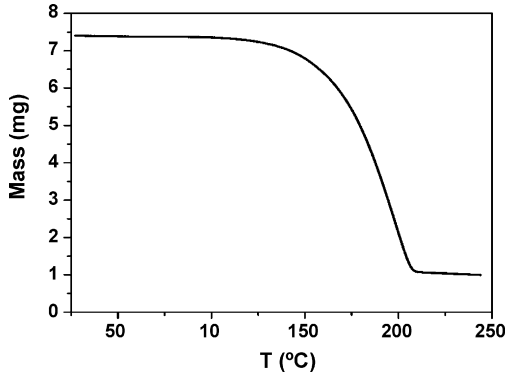

Fig. 8. TGA curve of liquid oleylamine in air, heating rate: 5 °C min^{-1}.

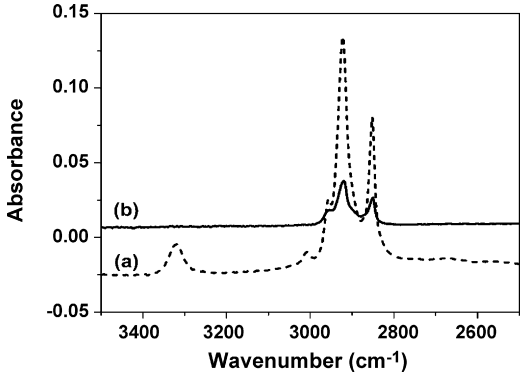

Fig. 9. FT-IR spectra of 4.0 nm Pt particles dispersion: (a) as-prepared and (b) after heat treatment in air at 185 °C for 5 h.

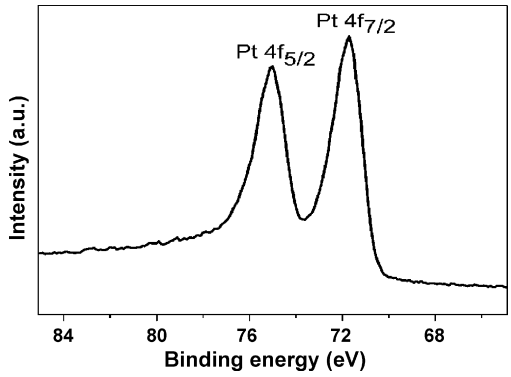

Fig. 10. XPS spectrum (Pt 4f) of 4.0 nm Pt particles after the heat treatment in air at 185 °C for 5 h.

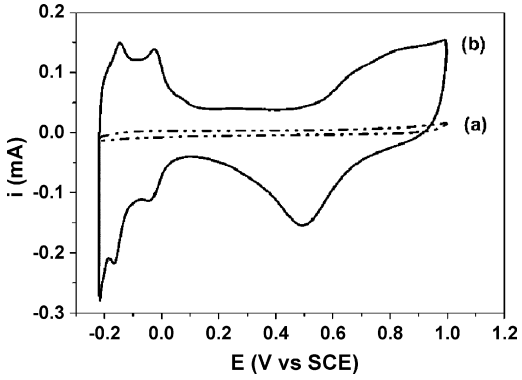

Fig. 11. Cyclic voltammogram of 4.0 nm Pt nanoparticles supported on Vulcan XC-72 in 1.0 M H_2SO_4: (a) as-prepared and (b) after heat treatment in air at 185 °C for 5 h. Scan rate: 50 mV s^{-1}.

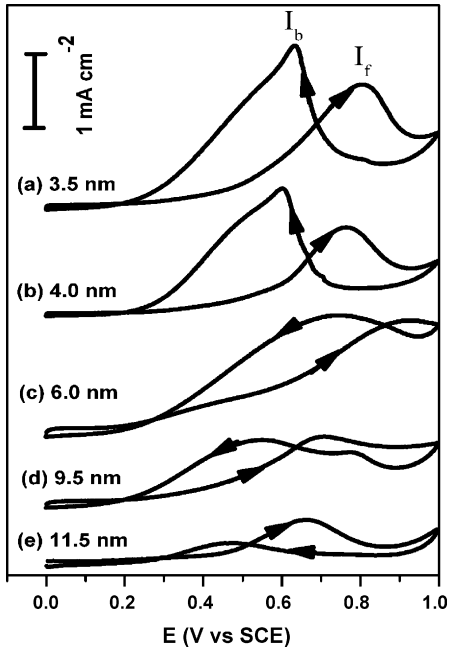

Fig. 12. Cyclic voltammograms of activated Pt particles supported on Vulcan XC-72 in 1.0 M H_2SO_4 + 2.0 M CH_3OH: (a) 3.5 nm particles, (b) 4.0 nm particles, (c) 6.0 nm particles, (d) 9.5 nm particles and (e) 11.5 nm particles. Scan rate: 50 mV s^{-1}. The *y*-axis is normalized current density in mA cm^{-2} and scale bar stands for 1 mA cm^{-2}.

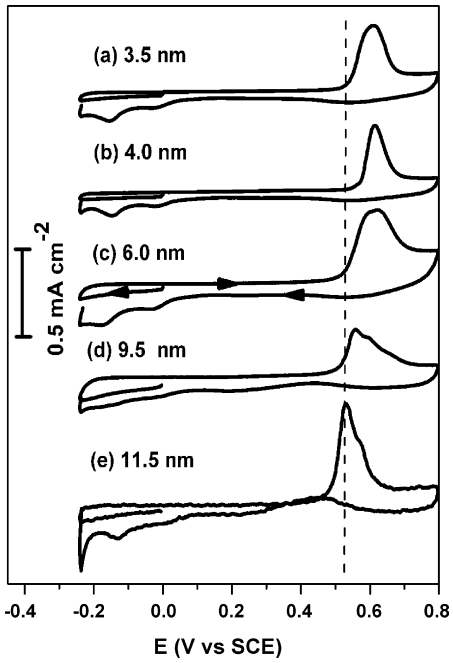

Fig. 13. CO-stripping curves of activated Pt nanoparticles supported on Vulcan XC-72: (a) 3.5 nm particles, (b) 4.0 nm particles, (c) 6.0 nm particles, (d) 9.5 nm particles and (e) 11.5 nm particles. Electrolyte: 1.0 M H_2SO_4. The *y*-axis is normalized current density in mA cm^{-2} and scale bar stands for 0.5 mA cm^{-2}. CO was pre-absorbed on Pt particle surface by bubbling the solution with CO for 5 min at 60 mV (vs. SCE). The CO dissolved in solution then was removed by purging the solution with N_2 for 30 min. The potential (*E* vs. SCE) was scanned: 0 mV → −240 mV → 800 mV → −240 mV. Scan rate: 50 mV s^{-1}.

size-dependent CO monolayer oxidation on Pt/C also was also observed in previous investigations [5,20,21], but the reason for this observation is still not fully understood. Friedrich et al. proposed that the positive shift of CO-stripping potential on big-size particles was likely attributed to the strong bonding of CO to the surface of small Pt particles and the concomitant decrease in CO diffusion and slow kinetics of OH groups generation [22,23]. Arenz et al. [5] suggested that the CO-stripping is mainly controlled the number of defects on the particles. They found the larger particles are smoother and contain more "irregularities" than smaller particles. The "irregularities" or "defects" can act as active sites for OH adsorption. It should be mentioned that the contribution of electronic effects may not be excluded for this size-dependent property, since the electronic effect and geometric effect of nanostructures are always interrelated to each other. This size-dependent tendency on CO monolayer oxidation is consistent with the size-dependent CO tolerance observed in methanol oxidation. All in all, for carbon-supported Pt nanocatalysts with different size, there is a compromise between the catalytic activity for methanol oxidation and CO adlayer oxidation.

4. Conclusion

Preparation of well-dispersed Pt nanoparticles with controlled size and narrow size distribution was achieved by the polyalcohol reduction of platinum acetylacetonate with the presence of oleylamine. Nearly monodispersed Pt particles were

obtained through a simple size selection method. High-loading (40%) carbon-supported catalysts were prepared by directly depositing Pt particles on Vulcan XC-72 carbon powder. The carbon-supported as-prepared particles could be catalytically activated by removing the oleylamine bound to the particle surface at low temperature (185 °C), without causing the aggregation and oxidation of particles. The heat-treated Pt particles exhibited considerably higher catalytic activity than as-prepared particles. Size-dependent study indicates the 3.5 nm and 4.0 nm Pt particles have a much higher intrinsic activity for methanol oxidation but a lower tolerance to CO poisoning, compared with 6.0 nm, 9.5 nm and 11.5 nm particles and the easiness for CO oxidation decreases with the decreasing of particle size. In all, this paper reported a new method for preparing and activating high-loading carbon-supported Pt nanocatalysts with controlled size, narrow size distribution and high electrocatalytic activity and the size-dependent catalytic activity of particles for methanol and CO oxidation was also investigated.

Acknowledgements

This work was supported by grant DE-FG02-01ER45867 from the U.S. Department of Energy. The project made use of the shared user instrumentation in the Center for Materials for Information Technology, a NSF Materials Research Science and Engineering Center (Award DMR 02-13985).

References

[1] T.S. Armadi, Z.L. Wang, T.C. Green, A. Henglein, M.A. El-Sayed, Science 272 (1996) 1924–1925.
[2] S. Park, Y. Xie, M.J. Weaver, Langmuir 18 (2002) 5792–5798.
[3] S. Mukerjee, J. Mcbreen, J. Electroanal. Chem. 448 (1998) 163–171.
[4] R. Narayanan, M.A. El-Sayed, Nano Lett. 4 (2004) 1343–1348.
[5] M. Arenz, K.J.J. Mayrhofer, V. Stamenkovic, B.B. Blizanac, T. Tomoyuki, P.N. Ross, N.M. Markovic, J. Am. Chem. Soc. 127 (2005) 6819–6829.
[6] W. Li, C. Liang, W. Zhou, J. Qiu, Z.H. Zhou, G. Sun, Q. Xin, J. Phys. Chem. B 107 (2003) 6292–6299.
[7] V. Lordi, N. Yao, J. Wei, Chem. Mater. 13 (2001) 733–737.
[8] Y. Xing, J. Phys. Chem. B 108 (2004) 19255–19259.
[9] M. Endo, Y.A. Kim, M. Ezaka, K. Osada, T. Yanagiswa, T. Hayashi, M. Terrones, M.S. Dresselhaus, Nano Lett. 3 (2003) 723–726.
[10] I. Lee, K.Y. Chan, D.L. Philips, Ultramicroscopy 75 (1998) 69–76.
[11] F. Gloaguen, J.M. Leger, C. Lamy, A. Marmann, U. Stimming, R. Vogel, Electrochim. Acta 44 (1999) 1805–1816.
[12] O.V. Cherstiouk, P.A. Simonov, E.R. Savinova, Electrochim. Acta 48 (2003) 3851–3860.
[13] J. Prabhuram, X. Wang, C.L. Hui, I.M. Hsing, J. Phys. Chem. B 107 (2003) 11057–11064.
[14] T. Kim, M. Takahashi, M. Nagai, K. Kobayashi, Electrochim. Acta 50 (2004) 817–821.
[15] T.J. Schmidt, H.A. Gasteiger, D.G. Stab, P.M. Urban, D.M. Kolb, R.J. Behm, J. Electrochem. Soc. 145 (1998) 2354–2358.
[16] Z. Liu, X.Y. Ling, X. Su, J.Y. Lee, J. Phys. Chem. B 108 (2004) 8234–8240.
[17] T. You, O. Niwa, T. Horiuchi, M. Tomita, Y. Iwasaki, Y. Ueno, S. Hirono, Chem. Mater. 14 (2002) 4796–4799.
[18] R. Woods, J. Electroanal. Chem. 49 (1974) 217–226.
[19] P.J. Ferreira, G.J. La O, Y. Shao-Horn, D. Morgan, R. Makharia, S. Kocha, H.A. Gasteiger, J. Electrochem. Soc. 152 (2005) A2256–A2271.
[20] M. Frederic, S.R. Elena, S.A. Pavel, Z.I. Vladimir, S. Ulrich, J. Phys. Chem. B 108 (2004) 17893–17904.
[21] K.J.J. Mayrhofer, B.B. Blizanac, M. Arenz, V.R. Stamenkovic, P.N. Ross, N.M. Markovic, J. Phys. Chem. B 109 (2005) 14433–14440.
[22] K.A. Friedrich, F. Henglein, U. Stimming, W. Unkauf, Electrochim. Acta 45 (2000) 3283–3293.
[23] K.A. Friedrich, F. Henglein, U. Stimming, W. Unkauf, Electrochim. Acta 47 (2001) 689–694.